Pyrenyl Fluorescence as a Probe of Polymer Structure and Diffusion in a Polyethylene:Poly(butyl methacrylate)-*co*-polystyrene Interpenetrating Network and Related Polymers

Csaba Kósa,[†,‡] Martin Danko,[†] Agnesa Fiedlerová,[†] Pavol Hrdlovic,[†] Eberhard Borsig,[†] and Richard G. Weiss*[,‡]

Polymer Institute, Slovak Academy of Sciences, Dúbravská cesta 9, 842 36 Bratislava, Slovak Republic, and Department of Chemistry, Georgetown University, Washington, D.C. 20057-1227

Received November 7, 2000; Revised Manuscript Received February 9, 2001

ABSTRACT: Dynamic and static photophysical and spectroscopic measurements have been used to analyze the microdomains of interpenetrating network (**IPN**) films consisting of 1:1 polyethylene:(7:3)-poly(butyl methacrylate)-*co*-polystyrene. The primary probe, fluorescence from pyrenyl groups covalently attached selectively to the different elements of the **IPN**, has been monitored under a variety of conditions, including in the absence and presence of a fluorescence quencher, diethyl oxalate (**DEO**), which is not able to enter domains of polyethylene. It has been possible to discern the parts of the **IPN** that are accessible to molecules of **DEO** and the rates at which **DEO** is able to enter them. Two diffusion coefficients, indicating parallel diffusion pathways, are necessary to account for **DEO** entry into several of the films. The **IPN** consists of largely segregated domains, but there are extensive interactions between domains at their interfaces. Conclusions are derived from comparisons of results from the **IPN** and films of their constituent polymeric elements when each is tagged with the lumophoric groups, as well as from films containing noncovalently linked pyrenyl groups. These results help to clarify the picture of the network derived from structural studies by providing dynamic insights into degrees of domain interpenetration and permeability.

Introduction

The syntheses, thermal properties, and dynamic-mechanical behavior of several interpenetrating network polymers (**IPN**)[1,2] consisting of low-density polyethylene (**LDPE**) and poly(butyl methacrylate)-*co*-polystyrene (**BMAcoS**) have been reported previously.[3] The networks are stabilized by cross-links between the polyethylene and poly(butyl methacrylate)-*co*-polystyrene segments. From electron micrographs (i.e., *static* measurements), ca. 0.1 μm thick sheaths of **LDPE** surround ca. 1 μm copolymer domains.[3,4] The structure of **BMAcoS** and a cartoon representation of the **IPN** networks are shown in Scheme 1.

Here, we use static and dynamic fluorescence measurements to investigate the micromorphology, selective permeability, and guest diffusion in one of these **IPN**s with the (molar) composition, 1:1 **LDPE**:(7:3)**BMAcoS**.[4] The probes (Scheme 1) are unattached (doped) and covalently bound pyrenyl or pyrenyl-derived groups that are located in specific segments of the network. Pyrenyl and related lumophoric groups have been linked covalently to the **LDPE** part of the **IPN** by a grafting technique[5] and to the butyl methacrylate−styrene (**BMAcoS**) copolymer part by copolymerization with 1-pyrenylmethyl methacrylate (**PYMA**) or 4-(1-pyrenyl)-methoxymethylstyrene (**PYS**). The dimensions of the microdomains are orders of magnitude too large for a detectable fraction of pyrenyl groups attached to one **IPN** component to be affected by the other if they are completely segregated as shown idealistically in Scheme 2.

Luminescence from pyrenyl groups[6] has been used here to investigate the micromorphological properties of these **IPN**s. Steady state and dynamic measurements of excited-state complex (excimer) formation can be correlated with local mobility and solubility characteristics of a polymer.[7−10] For instance, quantitative information about diffusion rates and permeability of dopant molecules can be obtained from fluorescence quenching

Scheme 1. Structures of Constituent Molecules Employed in This Work and a Cartoon Representation of a Two Dimensional Slice of an IPN

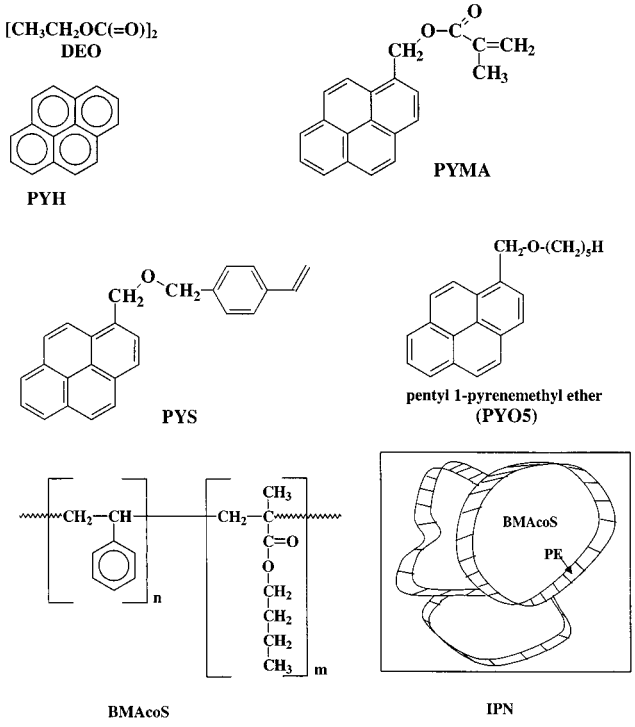

[†] Slovak Academy of Sciences.
[‡] Georgetown University.

10.1021/ma0019151 CCC: $20.00
Published on Web 03/16/2001

Scheme 2. Cartoon Representation of a Cross Section of an IPN with Covalently Attached Pyrenyl Groups: (a) PY−IPN; (b) PYMA−IPN or PYS−IPN

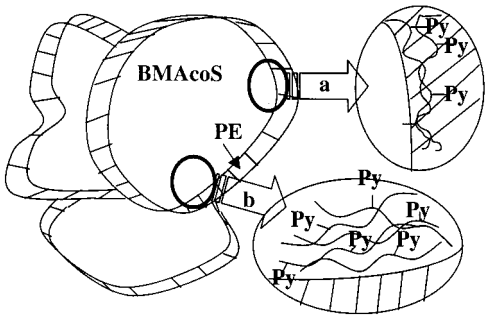

of interior-labeled polymer films,[5,11] and pyrenyl groups appended to film surfaces provide information about interfacial interactions with a liquid or gaseous phase.[12] Additionally, the ratio between the intensities of the first and third vibronic bands in emission (I_1/I_3)[13,14] can be used to characterize the local polarity of pyrenyl probe sites.[9,15] A combination of I_1/I_3 ratios and dynamic fluorescence decay measurements can provide still other features of polymer environments.[16,17] In this work, we have compared the static and dynamic fluorescence in selectively labeled **IPN** films and constituent films (i.e., **LDPE**, polystyrene (**PS**), poly(methyl methacylate) (**PMMA**), and **BMAcoS**) with doped or covalently attached pyrenyl groups (Table 1) to assess the degree of comingling of chains between **LDPE** and **BMAcoS** domains. These results have been augmented by changes induced in the fluorescence from covalently attached groups by a diffusive quencher, diethyl oxalate (**DEO**). It is shown that **DEO** can be a selective, sensitive tool for investigating micromophologically separated polymers.

Experimental Part

Instrumentation. UV/vis absorption spectra were recorded on a Perkin-Elmer Lambda-6 spectrophotometer using air as reference for polymer films. Emission spectra were obtained on a Spex Fluorolog spectrofluorimeter (linked to a personal computer) with a 150 W high-pressure xenon lamp using 0.25 mm slits for excitation and emission monochromators. Films in closed Pyrex cells (1 × 1 cm) were placed under a nitrogen atmosphere (circulated for 15 min), aligned at 45° to the incident radiation, and emission was detected at a right angle from the back-face. Excitation wavelengths (λ_{ex}), ∼345, ∼328, and 353 nm, corresponded respectively to the maxima of the first and second vibronic bands in absorption spectra and a small peak sometimes detectable in excitation spectra.

Fluorescence decay histograms were obtained with an Edinburgh Analytical Instruments model FL900 single photon counting instrument[18] using H_2 as the lamp gas. Emission was detected from the geometry indicated above. An "instrument response function" was determined using Ludox as scatterer. Solutions and films for some measurements were degassed in 4 mm thick Pyrex cuvettes on an Hg-free vacuum line using several freeze−pump−thaw cycles at $<10^{-5}$ Torr. Data were fitted to exponential functions and distribution algorithms using software supplied by Edinburgh. "Scatter" peaks of very short duration present in the decay profiles of the polymer films were used in the fits but are not reported. Distribution analyses were fitted by up to 100 exponential decays. Fitting was done with re-convolution and using additional time shifts to improve fitting. A grid technique was combined with the Marquardt procedure[19] to optimize the shifts and other parameters. Unless indicated otherwise, only fits from the distribution analysis method are reported. Relative percentages of each decay component are expressed as eq 1 in which τ_i is a decay constant and A_i is the associated preexponential factor.

$$\text{rel } \% = A_i\tau_i / \sum A_i\tau_i \qquad (1)$$

Materials. Diethyl oxalate (**DEO**; 99+%), 1-pyrenemethanol (98%), 1-iodopentane (98%), butyl methacrylate, and deuteriochloroform were from Aldrich. Toluene and dimethylformamide (from Mallinckrodt), and hexanes, ethyl acetate, methanol, and chloroform (from Fischer) were HPLC grade. They and styrene (Chemapol), divinylbenzene (Merck), and 2,5-dimethyl-2,5-di(*tert*-butylperoxy)hexane (Luperox 101; BASF) were used as received.

Synthesis of Pentyl 1-Pyrenemethyl Ether (PYO5).[16] 1-Pyrenemethanol (1.0 g, 4.3×10^{-3} mol) and 0.16 g (6.7×10^{-3} mol) of sodium hydride were dissolved in 20 mL of dimethylformamide with stirring under a dry atmosphere. 1-Iodopentane (0.65 mL, 5.0×10^{-3} mol) was added dropwise with stirring. After 15 h, 100 mL of distilled water was added, and a yellow solid was separated by filtration. After repeated recrystallizations from methanol, 0.5 g (41%) of product, mp (corr) 58.5−59.9 °C, was obtained. Only one peak was detected by HPLC analysis on a 250 × 4.6 mm 5 μm IBM Instruments silicagel column (95:5 (v:v) hexane:ethyl acetate) with UV/vis detection (254 and 376 nm).

Preparation of Polymer Films. General Polymerization Procedures. Polymerizations were conducted by heating monomeric solutions between glass plates sealed on the edges with PVC tubing. Concentrations of covalently attached pyrenyl groups were determined from UV/vis absorption spectra using the same molar extinction coefficient at 343 nm as for 1-ethylpyrene in hexane, 41 100 M^{-1} cm^{-1} and assuming film densities of 1 kg/dm^3. Average film thicknesses, from measurements with a micrometer at several positions on each film, and pyrenyl concentrations are listed in Table 1.

Polyethylene films, made by pressing low-density powder (BRALEN RA 2−19, Slovnaft, Bratislava) at 160 °C for 5 min at 35−40 kN, were doped with ca. 2.5×10^{-2} mol/kg pyrene (by swelling with a chloroform solution and selective removal of the liquid). Pyrenyl groups and another lumphore (vide infra) were covalently attached to the polyethylene by UV irradiation (λ > 300 nm; 1000 W high-pressure Hg lamp).[5] Removal of unattached pyrene by exhaustively soaking films in chloroform aliquots and drying yielded **PY−LDPE** films. The concentration of covalently attached lumophoric groups was estimated by UV/vis absorption spectroscopy. Translucent **PY−IPN** films were prepared by heating 2.8 g of **PY−LDPE** in 9.95 g (0.07 mol) of butyl methacrylate, 3.1 g (0.03 mol) of styrene, and a small amount of benzoquinone (to inhibit polymerization at this stage). 1,4-Butanediol dimethacrylate (1 mol %), and 2 wt % LUPEROX 101 were added. Polymerization was carried out at 110 °C for 6 h followed by 1 h at 160 °C.

Translucent **PYMA−BMAcoS** and **PYS−BMAcoS** films were prepared by a modification of a published procedure.[3,20] **PYMA** or **PYS** (10^{-4} mol/kg) was dissolved in a 7:3 molar ratio of butyl methacrylate and styrene. 1,4-Butanediol dimethacrylate (1 mol %) and 2 wt % LUPEROX 101 were added. The solution was heated at 110 °C for 6 h and 160 °C for 1 h.

Translucent **PYMA−IPN** and **PYS−IPN** films were obtained by a polymerization protocol (2 wt % LUPEROX 101; 110 °C for 6 h followed by 1 h at 160 °C) like that described to make **IPN**[3] from 10^{-4} mol/kg **PYMA** or **PYS** in 7/3 (mol/mol) butyl methacylate/styrene and 1 mol % 1,4-butanediol dimethacrylate in the presence of an "equimolar" amount of **LDPE**.

Translucent **PYMA−PBMA** films were prepared[3] from 10^{-4} mol/kg **PYMA** in butyl methacrylate and 2 wt % LUPEROX 101 at 85 °C for 24 h. Opaque **PYS−PS** films were obtained by heating 10^{-4} M **PYS** and 2 wt % LUPEROX 101 in **PS** at 110 °C for 6 h.

Preparation of pyrene-doped **IPN** and **BMAcoS** films, **PYH-IPN** and **PYH−BMAcoS**, respectively, followed the procedure to make the corresponding undoped films,[3] but in the presence of 10^{-4} mol/kg pyrene.

Table 1. General Description of Pyrenyl-Modified and Pyrenyl-Doped Films, Including Fluorescence Intensity Ratios (I_1/I_3) as Peak Heights ($I_1 \cong 376$ nm, $I_3 \cong 387$ nm, and $\lambda_{ex} \cong 345$ nm) from Pyrenyl Groups in N_2-Saturated Polymer Films (10^{-4} mol/kg)

film	description	[pyrenyl], mol/kg	av thickness (l), mm	I_1/I_3[c]
PY−LDPE	pyrene (**PYH**) covalently attached to **LDPE** by irradiation	ca. 3.7×10^{-4} [a]	0.25	0.60[d]
PYMA−BMAcoS	1-pyrenylmethyl methacrylate (**PYMA**) covalently attached to the **BMAcoS** (7:3) during copolymerization	10^{-4} [b]	2.1	1.26
PYS−BMAcoS	4-(1-pyrenyl)methoxymethyl styrene (**PYS**) covalently attached to **BMAcoS** (7:3) during copolymerization	10^{-4} [b]	2.1	0.97
PY−IPN	**IPN** made from **PY−LDPE**	ca. 6×10^{-6} [a]	1.9	0.50[d]
PYMA−IPN	**IPN** made from **PYMA−BMAcoS**	10^{-4} [b]	1.3	1.29
PYS−IPN	**IPN** made from **PYS−BMAcoS**	10^{-4} [b]	2.1	0.97
PYMA−PBMA	**PYMA** copolymer with butyl methacrylate (**BMA**)	10^{-4} [b]	2.8	1.51
PYS−PS	**PYS** copolymer with styrene (**S**)	10^{-4} [b]	3.2	0.70
PYH−BMAcoS	**PYH** doped in **BMAcoS** (3:7) copolymer by swelling in chloroform	10^{-4} [b]	2.1	1.04
PYH−IPN	**PYH** doped in **IPN** by swelling in chloroform	10^{-4} [b]	1.9	1.04
PYO5−PS	pentyl 1-pyrenemethyl ether (**PYO5**) doped in **PS** by casting a film from chloroform	10^{-4} [b]	0.054	1.21[e]
PYO5−PMMA	**PYO5** doped in **PMMA** by casting a film from chloroform	10^{-4} [b]	0.056	1.41

[a] From absorption spectra and Beer's law. [b] Concentration of pyrenyl groups added during polymerization or film casting. [c] Ratios for 10^{-4} mol/L **PYO5** are 0.73 in *n*-hexane, 1.21 in toluene, and 1.42 in ethyl acetate. [d] Contains an additional lumophore.[22] [e] 1.08 reported from **PYO6** in **PS**.[16]

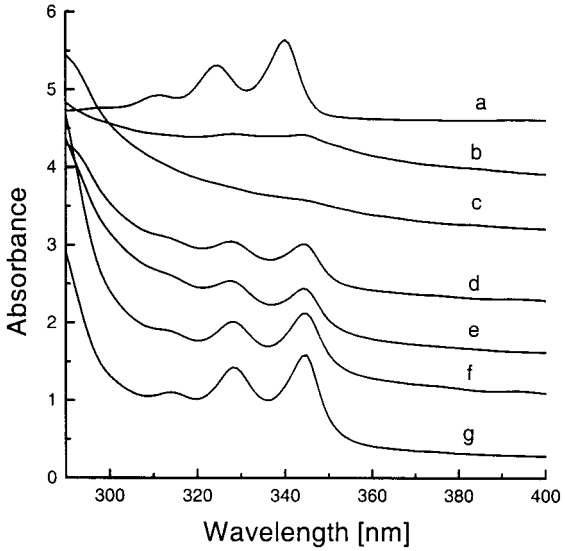

Figure 1. UV/vis absorption spectra of 7.9×10^{-6} mol/L **PYO5** in methanol (a) and films of **PY−LDPE** (b), **PY−IPN** (c), **PYS−IPN** (d), **PYMA−IPN** (e), **PYS−BMAcoS** (f), and **PYMA−BMAcoS** (g). The spectra are offset vertically.

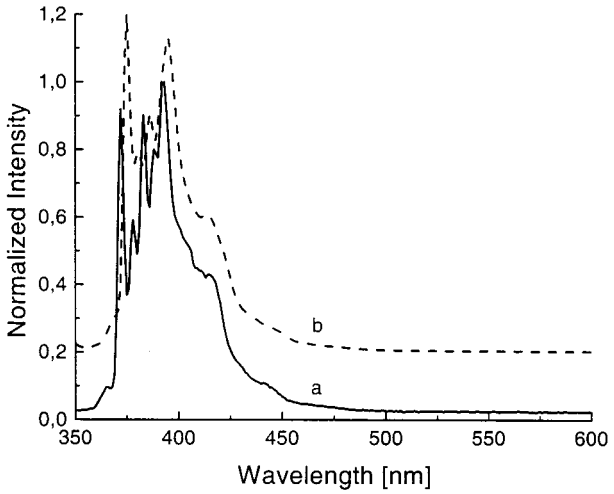

Figure 2. Steady-state emission spectra of 10^{-4} mol/kg **PYH** in **BMAcoS** (λ_{ex} 335 nm) (a) and **PYMA−IPN** (offset vertically, λ_{ex} 345 nm) (b).

PYO5-doped films, **PYO5−PS** and **PYO5−PMMA**, were prepared by dissolving 100 mg of polystyrene (**PS**; Avocado Research Chemicals, Ltd.; M_w 100 000, used as received) or poly(methyl methacrylate) (**PMMA**; Polysciences, Inc.; M_w 100 000, used as received) and 10^{-4} mol/kg of polymer of 1-**PYO5** in 2 mL of chloroform and casting the solution on a glass plate that was covered by a Petri dish in the dark to allow slow evaporation of the solvent. The dry, self-supporting films were separated from the glass plates by dipping into distilled water and placed under vacuum (<2 Torr) at ambient temperature for 5 h to remove residual solvent.

Results and Discussion

Steady-State Absorption and Emission Spectra. Typical absorption spectra of pyrenyl-labeled films and **PYO5** in methanol are plotted on the same absorbance scale in Figure 1. The electronic absorption of **PYO5** in the polar solvent methanol is slightly shifted hypsochromically with respect to that of the covalently attached pyrenyl groups in the polymers. When calculating chromophore concentrations (using Beer's law and assuming that the molar extinction coefficients are the same as that of **PYO5**), the absorbance scales of weakly absorbing films were expanded to increase precision. Even so, and although contributions to optical densities from reflection and diffraction of light by the films were subtracted prior to the calculations, the concentrations listed in Table 1 are only estimates; the exact concentrations are not necessary for our studies.

Vibronic features typical of fluorescence from a 1-pyrenyl group[13] were observed between 370 and 400 nm in emission spectra of films with covalently attached 1-pyrenemethoxy groups (Figure 2). Emission spectra from films prepared by irradiation of pyrene in **LDPE**[5] were dependent on λ_{ex} (Figure 3); a lumophore in addition to 1-pyrenyl groups was attached to the polymer chains.[21,22]

I_1/I_3 ratios[9,16,17,23] from **PYO5** are virtually the same in toluene and **PS** or in ethyl acetate and **PMMA**, as expected, and they are very similar to the ratios reported from hexyl 1-pyrenylmethyl ether in the same solvents.[16] However, ratios from 1-pyrenemethoxy groups covalently attached to polymer chains do not follow a predictable order (Table 1). Multiple environments of sites potentially occupied by the pyrenyl groups, related to film formation by casting from solvent and by cooling

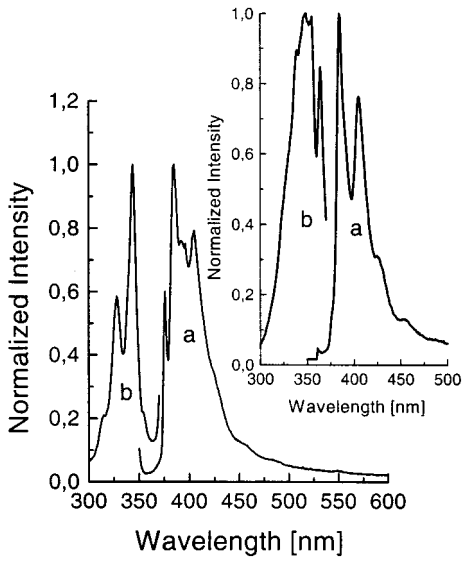

Figure 3. Steady-state emission and excitation spectra of **PY−LDPE** under a nitrogen atmosphere. (a) Emission spectra: λ_{ex} 345 and 353 nm (inset). (b) Excitation spectra: λ_{em} 376 and 384 nm (inset).

from a melt, must be present. The observed I_1/I_3 ratios are actually $\sum\chi_i I_{1i}/\sum\chi_i I_{3i}$ (where χ_i is the product of the mole fraction occupancy and quantum efficiency for emission in a site of type *i*).

Despite these complications, we conclude from I_1/I_3 ratios that the copolymerization process between butyl methacrylate and styrene leads to homo-chain segments into which the 1-pyrenemethoxy groups are incorporated selectively depending upon the nature of their polymerizable group from the observation that $I_1/I_{3(\mathbf{PYMA-BMAcoS})} > I_1/I_{3(\mathbf{PYS-BMAcoS})}$.

Pyrenyl groups prefer to reside within the **BMAcoS** parts of the **IPN**. Lumophoric groups remain sequestered within **BMAcoS** domains during formation of the interpenetrating networks with **LDPE**. The comparable, low ratios from **PY−LDPE**,[24] **PYH−LDPE**, *and* **PY−IPN**,[22] as well as the nearly identical appearances of emission spectra from **PY−LDPE** and **PY−IPN** (Supplementary Figure 1) and from **PYS−IPN** and **PYS−BMAcoS** (Supplementary Figure 2), indicate that lumophores attached to **LDPE** also remain within their original domains after the interpenetrating networks are established.

In both **PYS−BMAcoS** and **PYMA−BMAcoS** copolymers, the lowest energy vibronic band of the $S_2 \leftarrow S_0$ transitions of 1-pyrenemethoxy lumophores in excitation spectra are broadened and centered at ca. 344 nm. Because this wavelength is an intermediate value for the range of narrower bands from the constituent single-component polymers—346 (**PYO5−PS**), 342 (**PYO5−PMMA**), and 347 nm (**PYS−PS** and **PYMA−PBMA**)—the pyrenyl groups in **BMAcoS** appear to reside in more than one distinct environment.

Dynamic Fluorescence Decays from Model Lumophores and Modified Films. Decay constants (τ) from time-correlated single-photon-counting (TCSPC) experiments are independent of the spot on a film from which data are collected provided the same spot is interrogated throughout any one experiment. However, morphological inhomogeneities at different spots within a film may affect slightly the preexponential terms (and percent contributions) associated with the constants. For these reasons, films were held in fixed positions during collection of each data set.

Table 2. Fluorescence Decay Constants (τ), Their Relative Percentages (in Parentheses), and Goodness-of-Fit Parameters (χ^2) from Pyrenyl-Labeled N_2-Saturated Films at Ambient Temperature[a]

film	λ_{ex}, nm	λ_{em}, nm	τ, ns (rel %)
PY−LDPE	345	376	173 (72), 20 (23), 2 (5) $\chi^2 = 1.14$
	353	385	20 (58), 180 (27), 71 (10), 4 (5) $\chi^2 = 1.1$
PY−IPN	345	376	154 (52), 22 (48) $\chi^2 = 1.03$
	353	385	124 (23), 18 (77) $\chi^2 = 1.09$
PYMA−BMAcoS	345	376	204 (100) $\chi^2 = 1.17$
	353	396	203 (95), 39 (3), 8 (2) $\chi^2 = 1.1$
PYMA−IPN	345	376	216 (100) $\chi^2 = 1.05$
	353	396	194 (94), 53 (6) $\chi^2 = 1.02$
PYS−BMAcoS	345	376	191 (84), 9 (16) $\chi^2 = 1.17$
	353	397	185 (86), 46 (5), 9 (9) $\chi^2 = 1.18$
PYS−IPN	345	376	205 (99), 30 (1) $\chi^2 = 1.18$
	353	398	190 (91), 39 (4), 7 (5) $\chi^2 = 1.11$
PYS−PS	347	376	197 (99), 23 (1) $\chi^2 = 1.04$
PYMA−PBMA	347	376	205 (99), 27 (1) $\chi^2 = 1.075$

[a] Reported decay constants are from fits that did not include very short duration "scatter" peaks. Relative percentages (in parentheses) are from fits of the total histograms, but with renormalization to remove the scattering components.

The fluorescence decay curve of a nitrogen-saturated solution of 8×10^{-6} mol/L **PYO5** in methanol could be fitted essentially to a single decay function ($\tau = 288$ ns) (Supplementary Figure 3). When saturated with molecular oxygen, the same sample provided very weak fluorescence and $\tau = 2.4$ and 0.7 ns components of about equal importance. Resaturation of the sample with nitrogen gave $\tau = 194$ ns. From the oxygen solubility in methanol at 25 °C, 0.236 cm^3/cm^3 (= 0.011 mol/L),[25] and application of Berlman's method,[26] the rate constant for quenching the pyrenyl excited singlet states of **PYO5** by molecular oxygen, $k_q \sim 3 \times 10^{10}$ M^{-1} s^{-1}, is near to both the value reported for quenching of pyrene[27] and the self-diffusion limit in methanol.[27,28] There was no spectroscopic evidence for ground-state complexation between oxygen and **PYO5**.

Table 2 includes dominant long decay constants and the much shorter, minor component(s) (probably from polymer impurities), as well as the χ^2 fitting parameters (*precision* at one standard deviation), that result from analyses of fluorescence decay histograms from films with covalently attached lumophores. At λ_{ex} 345−347 nm (i.e., the 0−0 band of the $S_2 \leftarrow S_0$ transition) and λ_{em} 376 nm (i.e., the I_1 emission band), all of the histograms, except those from **PY−LDPE** and **PY−IPN**, could be fitted reasonably well to single-exponential functions with decay constants ~150−200 ns. These data are consistent with the single exponential decays and τ values ~200 ns obtained from histograms of **PYO5** in isotropic solvents in the absence of molecular oxygen and in **PMMA**[29] (Table 3). Analyses using a sum of exponential terms or a distribution analysis gave es-

Table 3. Fluorescence Decay Constants (τ), Their Relative Percentages (in Parentheses), and Goodness-of-Fit Parameters (χ^2) from 10^{-4} mol/L (Solutions) or 10^{-4} mol/kg (Films) PYO5 in Degassed Media at Ambient Temperature

polymer/solvent	λ_{ex}, nm	λ_{em}, nm	τ, ns (rel %)
hexane	347	375	200 (99), 14 (1) $\chi^2 = 1.07$
toluene	347	375	206 (100) $\chi^2 = 1.15$
ethyl acetate	347	375	229 (100) $\chi^2 = 1.19$
PS	343	375	196 (99), 24 (1) $\chi^2 = 1.03$
PMMA	342	375	201 (100) $\chi^2 = 1.09$

Table 4. Fluorescence Decay Constants (τ), Their Relative Percentages (in Parentheses), and Goodness-of-Fit Parameters (χ^2) from Pyrenyl-Labeled N_2-Saturated Films Immersed in Various Neat Liquids at Ambient Temperature[a]

polymer	immersion time, h	λ_{ex}, nm	λ_{em}, nm	τ, ns (rel %)	$\langle t \rangle$,[b] ns
PY−**LDPE** immersed in ethyl acetate	0[b]	346	377	147 (60), 22 (40) $\chi^2 = 1.19$	97
	0.5	346	377	137 (64), 20 (36) $\chi^2 = 1.1$	95
	24	346	377	140 (65), 22 (35) $\chi^2 = 1.07$	99
PY−**LDPE** immersed in **DEO**	0[b]	346	377	147 (60), 22 (40) $\chi^2 = 1.19$	97
	0.5	346	377	157 (64), 23 (36) $\chi^2 = 1.05$	109
	90	346	377	158 (67), 22 (33) $\chi^2 = 1.18$	113
PYS−**BMAcoS** immersed in decane	0[c]	345	376	191 (84), 9 (16) $\chi^2 = 1.17$	162
	0.5	345	376	196 (97), 43 (3) $\chi^2 = 1.07$	191
	24	345	376	179 (96) 20 (4) $\chi^2 = 1.08$	173

[a] Reported decay constants are from fits that did not include very short duration "scatter" peaks. Relative percentages (in parentheses) are from fits of the total histograms, but with renormalization to remove the scattering components. [b] Weighted average of decay constants, $\sum \%_i \tau_i$. [c] Dry film.

sentially the same results; the distribution analyses are included in Table 4.

Generally, data sets from λ_{ex} 353 nm were more complex due to excitation of a greater fraction of polymer impurities, but only decays from the aforementioned **PY**−**LDPE** and **PY**−**IPN** films are dependent on λ_{ex} within the limits of *accuracy*. The oxidized lumophoric groups[21] in the latter films have much shorter τ values, ~20 ns, than that of pyrenyl. In addition, the relatively short τ value for the longer component of the **PY**−**IPN** sample excited at 353 nm is probably less precise than the low χ^2 indicates; due to signal-to-noise problems, the fitting routine cannot find a very accurate fit to a long decay when most of the data is in the early time channels.

Since the range of the pyrenyl decay constants is small (all are near 200 ns), they provide less information than the (static) I_1/I_3 ratios about the probe locations within the various components of the **IPN**. However, the similarity between the decay constants for **PYO5** and the 1-pyrenemethoxy groups linked to the polymer films provides strong evidence that the covalently bound lumophores do not reside in sites with exceptional characteristics. In addition, the decay constants should be much more responsive to the presence of fluorescence quenchers in different parts of the **IPN** than the I_1/I_3 ratios.

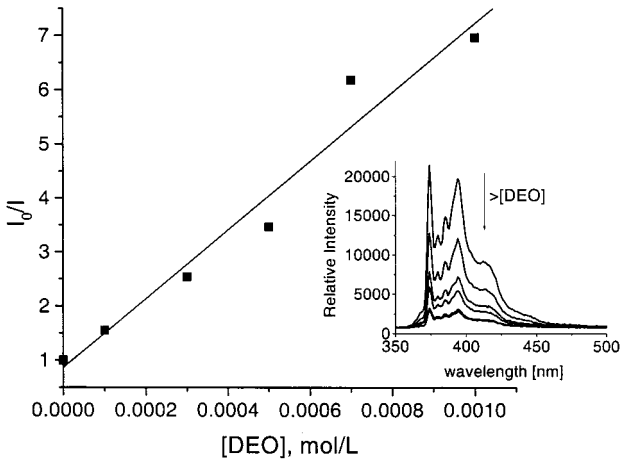

Figure 4. Fluorescence quenching of 7.9×10^{-6} mol/L **PYO5** in methanol by **DEO** (λ_{ex} 343, λ_{em} 374) according to the Stern−Volmer equation. Emission spectra upon which the data points are based are shown in the inset.

Selective Swelling of Covalently Linked Pyrenyl Groups in Films. To introduce quenchers of pyrenyl fluorescence selectively into the different parts of the **IPN** network, we attempted first to find a liquid that dissolves neither **LDPE** nor **BMAcoS** *but swells only one of the two.*

Decane, a swelling solvent for **PE**, was inappropriate for the **IPN**. Although steady-state emission spectra of **PYS**−**BMAcoS** were not changed perceptibly when immersed in decane and the longest (dominant) fluorescence decay constant was reduced only slightly (Table 4), the film was partially dissolved. In fact, no appropriate solvent for selective swelling exclusively the polyethylene component of the **IPN** was found. Attempts to swell only the **BMAcoS** part of the **IPN** with ethyl acetate, a poor solvent for polyethylene,[30,31] were unsuccessful as well. Although the permeability of ethyl acetate in **LDPE** at ambient temperature is reported to be 1 g/0.001cm/100cm^2/24 h[32] and immersion of **PY**−**LDPE** for 24 h in it caused practically no change in the emission spectra or decay characteristics (Table 4), the film was partially dissolved again.

Finally, diethyl oxalate (**DEO**), a solvent whose permeability to polyethylene is reported to be only 0.043 g/0.001cm/100cm^2/24 h,[32] swelled perceptibly and partially dissolved **BMAcoS**, but not our **LDPE**. We have been unable to find a literature value for the permeability of **DEO** to **PS** and **PBMA**. As expected from our visual inspection, the appearance and excitation wavelength dependence of emission spectra from **PY**−**LDPE** films, as well as their decay characteristics (vide infra), were unaffected by immersion in neat **DEO**. On this basis, we assume that the swelling detected in **IPN** films immersed in **DEO** is segregated in the **BMAcoS** parts.

Fluorescence Quenching of PYO5 by Diethyl Oxalate (DEO). Fortuitously, **DEO** is also an extremely efficient quencher of pyrenyl excited singlet states. A Stern−Volmer plot[33] (eq 2) of **PYO5** fluorescence intensity at 375 nm in N_2-saturated methanol (I_0) and in the presence of different concentrations of **DEO** (I) is shown with the best linear fit (K_D = 6770 M^{-1}; correlation coefficient = 0.979) in Figure 4. The inset spectra lack any apparent exciplex emission. Since

Table 5. Fluorescence Decay Constants (τ), Their Relative Percentages (in Parentheses), and Goodness-of-Fit Parameters (χ^2) from Degassed Pyrenyl-Labeled Films Immersed in Various DEO Solutions at Ambient Temperature[a]

film	immersion time, h	λ_{ex}, nm	λ_{em}, nm	τ, ns (rel %)	$\langle\tau\rangle$,[b] ns
PY−LDPE immersed in 1 M **DEO** in ethyl acetate	0.5	345	375	188 (62), 55 (10), 18 (23), 4 (5) $\chi^2 = 1.18$	126
	24	345	375	180 (63), 34 (20), 13 (14), 4 (3) $\chi^2 = 1.22$	122
PY−LDPE immersed in 1 M **DEO** in decane	0.5	345	375	161 (64), 20 (26), 4 (10) $\chi^2 = 1.05$	109
	24	345	375	174 (72), 20 (25), 3 (3) $\chi^2 = 1.19$	130
PYS−BMAcoS immersed in 1 M **DEO** in decane	0.5	345	375	201 (79) 58 (18), 11 (3) $\chi^2 = 1.11$	170
	24	345	375	85 (96), 9 (4) $\chi^2 = 1.05$	82
PYS−BMAcoS immersed in 1 M **DEO** in ethyl acetate	0.5	345	375	165 (51), 45 (42), 11 (7) $\chi^2 = 1.21$	104
	24	345	375	98 (9), 37, (79), 11 (12) $\chi^2 = 1.14$	39

[a] Reported decay constants are from fits that did not include very short duration "scatter" peaks. Relative percentages (in parentheses) are from fits of the total histograms, but with renormalization to remove the scattering components. [b] Weighted average of decay constants, $\Sigma\%_i\tau_i$.

PYO5 follows Beer's law ($\epsilon_{340} = 38\,800$ M^{-1} cm^{-1}) throughout the concentration ranges employed and **DEO** does not alter its absorption spectrum, ground-state complexes, if present, are not detectable spectroscopically. A collisional quenching mechanism is indicated, and the data (taking $\tau_0 = 288$ ns) give $k_q = 2.4 \times 10^{10}$ M^{-1} s^{-1}, near the diffusion-controlled limit.[28]

$$I_0/I = 1 + K_D[\mathbf{DEO}] = 1 + k_q\tau_0[\mathbf{DEO}] \qquad (2)$$

DEO Quenching of Fluorescence from Covalently Attached Lumophores in IPN and Related Polymers. Time-correlated single-photon-counting fluorescence decay profiles were also recorded for **PYS−BMAcoS** and **PY−LDPE** films immersed for short and long periods in degassed solutions of 1 M **DEO** in decane and ethyl acetate (Table 5). Significant fluorescent quenching by **DEO** (that increased slowly with immersion time) was detected from **PYS−BMAcoS** films in either ethyl acetate or decane solutions. As expected, the fluorescence decays of **PY−LDPE** were unaffected by prolonged immersion in ethyl acetate, a nonswelling medium for **PE**. However, **PY−LDPE** films were nearly equilibrated with **DEO** in decane solutions after only ca. 30 min of immersion. Since only a very small amount of **PY−LDPE** quenching occurs after protracted immersion periods, penetration by **DEO**, even when entrained by a good swelling solvent like decane, is slight!

In addition, "steady-state" fluorescence intensity changes were used to monitor the temporal course of the diffusion of neat **DEO** into several of the films at 50 °C.[5] As mentioned, steady-state fluorescence intensities are constant with time in the absence of a diffusing quencher provided the same spot is illuminated throughout. In the presence of a diffusing quencher, the fluorescence intensity of a stationary sample decreases with time at an interrogation spot.[5,34] Due to the nature of the experimental procedures, it was not possible to exclude air during these experiments. However, its presence does not affect the kinetics of diffusion of the **DEO** when films are immersed in it.

Data from plots like that shown in Figure 5 could not be fitted well to a normal integrated form of Fick's second law (eq 3[35]) in which the infinite series is truncated after the first 16 terms; χ^2 values were extremely high. The problem is not in the truncation,[35] but in the form of the equation. By using eq 4 (in which two diffusion pathways operate in parallel) and allowing D_1, D_2, and f_{D1} (a term indicating the relative importance of each of the diffusional processes) to be varied simultaneously, it was possible in most cases to obtain excellent fits.

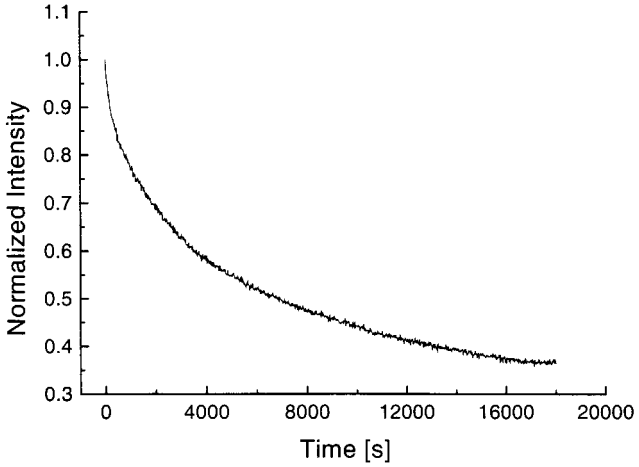

Figure 5. Temporal dependence of the normalized emission intensity from **PYMA−PBMA** immersed in 2 mL air-saturated **DEO** at 50 °C (λ_{ex} 347 nm, λ_{em} 377 nm).

$$\frac{I_t - I_\infty}{I_0 - I_\infty} = \frac{8}{\pi^2}\sum_{n=0}^{15}\frac{1}{(2n+1)^2}e^{-D(2n+1)^2\pi^2 t/l^2} \qquad (3)$$

$$\frac{I_t - I_\infty}{I_0 - I_\infty} = \frac{8}{\pi^2}\left\{f_{D_1}\sum_{n=0}^{15}\frac{1}{(2n+1)^2}e^{-D_1(2n+1)^2\pi^2 t/l^2} + (1 - f_{D_1})\sum_{n=0}^{15}\frac{1}{(2n+1)^2}e^{-D_2(2n+1)^2\pi^2 t/l^2}\right\} \qquad (4)$$

In these equations, C_t/C_0, the ratio of pyrenyl groups without a nearby **DEO** quencher at times t and 0, can be replaced by $(I_t - I_\infty)/(I_0 - I_\infty)$, where I_0, I_t, and I_∞ are fluorescence intensities after immersion of a film into **DEO** for times 0, t, and ∞ (i.e., when the intensity decreased incrementally by <1% during a 30 min

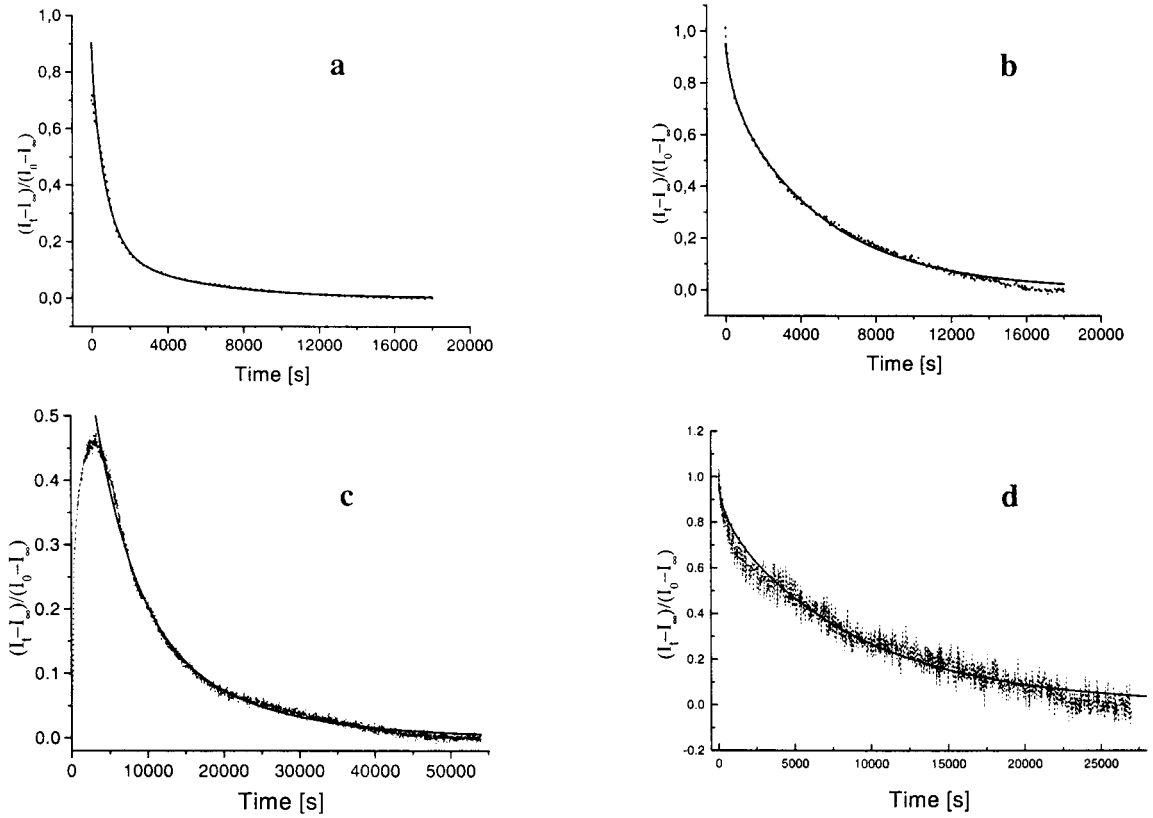

Figure 6. Plots of$(I_t - I_\infty)/(I_0 - I_\infty)$ vs time (...) for films immersed in 2 mL of **DEO** at 50 °C) and the best fit to eq 3 (d) or 4 (a−c) (—): (a) **PYMA−PBMA** using the data in Figure 5; (b) **PYMA−BMAcoS**; (c) **PYMA−IPN**; (d) **PY−IPN**.

Table 6. Fluorescence Intensity Ratios ($(I_0 - I_\infty)/I_0$), Diffusion Coefficients (D) of Neat DEO at 50 °C, and Film Masses before (M_1) and after (M_2) Immersion in 2 mL Neat DEO[c]

film	D_1, cm²/s (f_{D_1})	D_2, cm²/s ($1 - f_{D_1}$)	χ^2(reduced)	$(I_0 - I_\infty)/I_0$[b]	M_1, mg	M_2, mg[b]
PYS−PS	1.54×10^{-6} [a]		5.7×10^{-4}	0.89	127	film dissolved
PYMA−PBMA	$(1.15 \pm 0.16) \times 10^{-5}$ [a] (6.5%)	$(1.54 \pm 0.008) \times 10^{-6}$ [a] (93.5%)	1.6×10^{-4}	0.63	255	film dissolved
PYMA−BMAcoS	$(5.90 \pm 0.11) \times 10^{-6}$ (77.8%)	$(9.42 \pm 0.30) \times 10^{-7}$ (22.2%)	3×10^{-4}	0.96	210	350
PYS−BMAcoS	$(1.11 \pm 0.01) \times 10^{-5}$ (64%)	$(1.12 \pm 0.01) \times 10^{-6}$ (36%)	3.8×10^{-5}	0.90	248	430
PYMA−IPN	$(3.58 \pm 0.39) \times 10^{-7}$ (68%)	$(1.29 \pm 0.02) \times 10^{-7}$ (32%)	7×10^{-5}	0.74	95.7	92.7
PYS−IPN	4.42×10^{-7}		3.3×10^{-4}	0.71	160	141
PY−IPN	4.04×10^{-7}		2×10^{-3}	0.32	179	104

[a] A combination of diffusion into unswelled films and diffusion accelerated by swelling and dissolution. See text. [b] After 10 h at 50 °C and 2 weeks at ambient temperature immersed in neat **DEO**. [c] All measurements made in air. See text for additional details.

period); l is the film thickness (Table 1) and D is a diffusion coefficient for **DEO**.[35] Due to the manner in which films were immersed into **DEO** solutions, the precise I_0 value is unknown, and data taken within the first 60 s do not follow eq 3 or 4. To overcome these problems, the values of I_0 were calculated from the extrapolated intercepts of the linear portions of plots of fluorescence intensity vs $t^{1/2}$.[35] Representative plots of $(I_t - I_\infty)/(I_0 - I_\infty)$ vs time and best-fit lines using eq 3 or 4 are presented in Figure 6 and Supplementary Figures 4−6; the corresponding diffusion coefficients are collected in Table 6. Unfortunately, the numbers for **PYS−PS** and **PYMA−PBMA** cannot be interpreted as accurate diffusion coefficients. The loss of 1-pyrenemethoxy fluorescence intensity with time is due to a combination of quenching and partial dissolution (and swelling) of the films, both induced by **DEO**. Degradation of the films becomes more severe after longer contact times with **DEO**.

The $(I_0 - I_\infty)/I_0$ ratios in Table 6 are the fraction of lumophoric pyrenyl groups in the various films that are able to accommodate at least one molecule of **DEO** within their cavity sites under our equilibration conditions. As indicated from the previously described swelling experiments, parts of the **IPN** that are **PS**- or **PBMA**-enriched are much more permeable to **DEO** than the **LDPE**-rich parts. In fact, the ca. one-third of lumophoric groups quenched by **DEO** in **PY−IPN**, combined with the almost total lack of quenching in **PY−LDPE**, suggests that preparation of the **IPN** networks either brings some of the lumophores appended to polyethylene chains into regions containing **BMAcoS** chains or the swelling attendant to the **DEO** permeation experiments makes the environment around lumophores even in the **PE** regions appear more homogeneous. The similarity between the I_1/I_3 fluorescence intensity ratios from **PY−LDPE** (0.60) and **PY−IPN** (0.50), *measured at room temperature in unswelled films*, is consistent only with the latter hypothesis (as depicted in Scheme 2). If a large fraction of the **PY−IPN** lumophores were exposed to the **BMAcoS** part of the **IPN** network in the unswelled film, the I_1/I_3 ratio should be much larger than it is.

The influence of swelling is especially evident in the diffusional data for **PYMA−BMAcoS** (Figure 6b) and **PYS−BMAcoS** (Supplementary Figure 5). The excel-

Table 7. Fluorescence Decay Constants (τ), Their Relative Percentages (in Parentheses), and Goodness-of-Fit Parameters (χ^2) from Degassed Films at Ambient Temperature before and after Saturation with Neat DEO[a]

film	λ_{ex}, nm	λ_{em}, nm	τ_0, ns (rel %) before saturation	τ_0, ns (rel %) after saturation[b]	$\langle\tau_0\rangle/\langle\tau\rangle$[c]	I_0/I[d]
PY−PS[e]	347	377	200 (98), 57 (2) $\chi^2 = 1.19$	48 (19), 19 (36), 5 (46) $\chi^2 = 1.41$	10.9	9.1
PYMA−PBMA[e]	347	377	225 (99), 5 (1) $\chi^2 = 1.095$	11 (100) $\chi^2 = 1.15$	20.3	2.7
PYMA−BMAcoS	345	376	219 (96), 56 (4) $\chi^2 = 1.13$	29 (100) $\chi^2 = 1.02$	7.3	25
PYS−BMAcoS	345	376	218 (92), 69 (6), 10 (2) $\chi^2 = 1.05$	78 (24), 28 (32), 8 (44) $\chi^2 = 1.04$	6.6	10
PYMA−IPN	345	376	224 (95), 64 (5) $\chi^2 = 1.05$	101(34), 38 (48), 11 (18) $\chi^2 = 1.09$	4.0	3.8
PYS−IPN	345	376	206 (97), 42 (3)[f] $\chi^2 = 1.048$	50 (36), 21 (40), 9(11), 4 (13) $\chi^2 = 1.13$	7.2	3.4
PY−IPN	345	376	204 (69), 27 (31) $\chi^2 = 1.17$	158 (51), 20 (49) $\chi^2 = 1.21$	1.7	1.5

[a] Reported decay constants are from fits that did not include very short duration "scatter" peaks. Very short duration "scatter" peaks were present in the decay profiles. [b] 10 h at 50 °C and ≥2 weeks at ambient temperatures in neat **DEO**. [c] $\sum\%_{i0}\tau_{i0}/\sum\%_i\tau_i$ (i.e., the ratio of the weighted sums of the decay constants before and after saturation with **DEO**). [d] Ratio of emission intensities before and after saturation of films by **DEO**. [e] The decay constants are from pyrenyl groups in the films and dissolved by the **DEO**. See Table 6. [f] A very minor component of an extremely long decay component (>400 ns) is not included.

lent fits to eq 4 are based on sampling at least 90% of the lumophoric groups, and the D_1, D_2, and f_{D_1} values are very similar in the two films. The lack of microsegregation of 1-pyrenemethoxy groups into **BMA**- or **S**-enriched regions implied by the diffusional data is not consistent with the I_1/I_3 fluorescence ratios for the same films (Table 1). **DEO**-induced swelling of the films seems to mask the influence of microsegregation in the **BMAcoS** copolymer on the dynamic processes, as well as to lead to significant changes in its morphology. In addition, the rise in the early-time portions of the diffusional curves for **PYMA−IPN** (Figure 6c)[36] and **PYS−IPN** (Supplementary Figure 6) is not due to poor temperature equilibration or small movements of the films when **DEO** was initially added; it was found in these films only. We suspect that the initial contact with **DEO** causes subtle changes to the **BMAcoS** morphology, where the 1-pyrenemethoxy groups of these **IPN**s reside.

Good fits to eq 3 (i.e., one diffusion coefficient) from **PY−IPN** data (Figure 6d) or the decay portion of curves from **PYS−IPN** were possible. Although the permeability of **LDPE** to **DEO** is very small at ambient temperature, it must be larger at 50 °C. Regardless, comparisons of the data in Table 6 demonstrate that the specific locations of the covalently attached lumophores within the three derivatized **IPN** are not very important in determining the rate at which **DEO** molecules access them. However, these conclusions are based on the ca. three-fourths of the **PYS−IPN** and **PYMA−IPN** lumophores but only ca. one-third of the **PY−IPN** lumophores that participate in the **DEO** diffusional measurements. The environments of the remaining unquenched lumophores are not sampled on a steady-state basis by the **DEO**. Thus, it may be more accurate to state that swelling attendant to **DEO** diffusion and permeation makes all of the *accessed* environments within the interpenetrating network more or less kinetically indistinguishable, but the fraction of *inaccessible* environments is much greater within the **LDPE** part than within the **BMAcoS** part.

Dynamic fluorescence decay constants, as determined from distribution analyses from films in the absence of **DEO** and after prolonged immersion in it, were measured by TCSPC (Table 7). As indicated above, data from films that dissolved partially when immersed in **DEO** solutions, especially **PYS−PS** and **PYMA−PBMA**, cannot be interpreted rigorously.

In one model, all quenching in the films is static, the environments around lumophores lacking a molecule of **DEO** in their site cavities at the moment of electronic excitation are unaffected by the presence of **DEO** in other parts of a polymer, and **DEO** molecules have equal access to all lumophore-occupied site types. In such a case, (1) the values of τ should beindependent of the duration films are exposed to **DEO** (i.e., $\tau_0 = \tau$), (2) the fraction of each component of decay before and after **DEO** saturation should not change, and (3) the overall emission intensity should decrease as **DEO** equilibrates with a film (i.e., I_0/I should increase). Since only the third of these predictions is observed, the model must be modified. The fact that $\tau_0 \gg \tau$ and the fraction of each decay component changes implies that some quenching is dynamic and/or the sites of lumophores that lack a **DEO** molecule are still affected by the polymer bulk. The absence of exciplex emission from solutions of pyrenyl groups in **DEO** makes differentiation between static and dynamic quenching difficult. However, since the **BMAcoS** component of the **IPN** is swelled by **DEO**, it is reasonable to assume that the environments of nonquenched lumophores in swelled films may be very disturbed in ways that facilitate return of excited singlets nonradiatively to their ground states.

According to simple Stern−Volmer kinetics in an *isotropic* environment and in the absence of static quenching, the ratios of fluorescence intensities and decays (expressed in Table 7 as the ratio of weighted averages) should be equal: $I_0/I = \langle\tau_0\rangle/\langle\tau\rangle$. Such a data treatment is not appropriate here for several reasons: some of the films were partially dissolved during the incubation period with **DEO**; at the conclusion of the incubation period, quenching occurs in a mixture of isotropic and anisotropic environments. Also, comparison of the film weights before ($\mathbf{M_1}$) after ($\mathbf{M_2}$) incubation (Table 6) demonstrates that in several cases more film was dissolved than **DEO** was absorbed. Regardless, the similarity between the I_0/I ($\approx I_0/I_\infty$) and $\langle\tau_0\rangle/\langle\tau\rangle$ ratios in Table 7 for the **IPN** films suggests that a large fraction of the quenching is dynamic, and the absence of any vestiges of the τ_0 decay constant in the **DEO**-

saturated **IPN** films demonstrates that none of the lumophoric sites, including those in the **LDPE** domains, is totally isolated from the secondary effects of **DEO** swelling. However, the relatively small decreases in the τ and $\langle\tau\rangle$ values for the **PY**−**IPN** film indicate that its lumophores have limited exposure to **DEO** and to the substantial effects **DEO** has on the non-**PE** parts of the network. Since the perturbations by **DEO** to the environments experienced by the lumophores of the corresponding homopolymer, **PY**−**LDPE**, are much smaller still (Table 5), again we conclude that creation of an **IPN** network leads to significant changes to all of its parts.

Conclusions. In the absence of the swelling agent, diethyl oxalate (**DEO**), the local polarity in different microdomains of the **IPN** has been ascertained from the luminescence of both covalently attached and doped pyrenyl groups to be very similar to that of the corresponding polymer components. Measurements of the permeability to and swelling of lumophoric sites by **DEO** indicate that the **BMAcoS** and **LDPE** domains remain separated for the most part within the networks, at least at the micron scale, but chains intermingle near domain boundaries. Swelling (and quenching) by **DEO** is limited primarily to the **BMAcoS** portions of the networks; domains of the network are affected relatively selectively. The observation that two diffusion coefficients are necessary to account for **DEO** entry into several of the films indicates that parallel diffusion pathways to the pyrenyl probes are operative.

Overall, the *dynamic* picture that emerges is consistent with the reported *static* microstructure depicted in Scheme 2.[3,4] Even at superambient temperatures, the **IPN** retains its segregated nature over time in the presence of the swelling agent. Although the gross conclusions derived from the structural and dynamic measurements are the same, they provide complementary information: "segregated domains" has a somewhat different meaning when defined according to structural and dynamic parameters.

It will be interesting in future work to determine at what temperature the domains lose their individuality and to what extent they resegregate after cooling. The presence of covalently attached lumophoric groups, as used here, should allow these questions to be answered.

Acknowledgment. Authors from the Polymer Institute thank VEGA (Project 2/7009/20) for financial support. Authors from Georgetown are grateful to the National Science Foundation and the donors of the Petroleum Research Fund, administered by the American Chemical Society, for their support of this research. This article is dedicated to Professor Vaclav Horak in anticipation of his 80th birthday.

Supporting Information Available: Figures showing steady-state emmission spectra, dynamic fluroesence decay curves, and $(I_t - I_\infty)/I_0 - I_\infty)$ vs time. This material is available free of charge via the Internet at http://pubs.acs.org.

References and Notes

(1) Sperling, L. H. *Interpenetrating Polymer Network and Related Materials*; Plenum Press: New York, 1981.
(2) Klempner, D. *Angew. Chem., Int. Ed. Engl.* **1978**, *17*, 97.
(3) Greco, R.; Fiedlerová, A.; Schulze, U.; Borsig, E. *J. Macromol. Sci.—Pure Appl. Chem.* **1995**, *A32*, 1957.
(4) Borsig, E.; Hrouz, J.; Fiedlerová, A.; Ilavský, M. *J. Macromol. Sci.—Chem.* **1990**, *A27*, 1613.
(5) Naciri, J.; Weiss, R. G. *Macromolecules* **1989**, *22*, 3928.
(6) Hrdlovic, P.; Chmela, Š. *J. Photochem. Photobiol. A: Chem.* **1998**, *118*, 137.
(7) Avis, P.; Porter, G. *J. Chem. Soc., Faraday Trans. 2* **1974**, *70*, 1057.
(8) Szadkowska-Nicze, M.; Wolszczak, M.; Kroh, J.; Mayer, J. *J. Photochem. Photobiol. A: Chem.* **1993**, *75*, 125.
(9) Itaya, A.; Matsumoto, Y.; Iou, I.; Masuhara, H.; De Schryver, F. C. *Polymer* **1994**, *35*, 3920.
(10) Ying Chu, D.; Thomas, J. K. *Macromolecules* **1990**, *23*, 2217.
(11) Frank, R. S.; Merkle, G.; Gauthier, M. *Macromolecules* **1997**, *30*, 5397.
(12) Bergbreiter, D. E.; Gray, H. N.; Srinivas, B. *Macromolecules* **1994**, *27*, 7294.
(13) Dong, D. C.; Winnik, M. A. *Photochem. Photobiol.* **1982**, *35*, 17.
(14) Kalayanasundaram, K.; Thomas, J. K. *J. Am. Chem. Soc.* **1977**, *99*, 2039.
(15) Prado, E. A.; Yamaki, S. B.; Atvars, T. D. Z.; Zimerman, O. E.; Weiss, R. G. *J. Phys. Chem.* **2000**, *104*, 5905.
(16) Nakashima, K.; Winnik, M. A.; Dai, K. H.; Kramer, E. J.; Washiyama, J. *Macromolecules* **1992**, *25*, 6866.
(17) Zhao, C.-L.; Winnik, M. A.; Riess, G.; Croucher, M. D. *Langmuir* **1990**, *6*, 514.
(18) O'Connor, D. V.; Phillips, D. *Time-Correlated Single Photon Counting*; Academic Press: London, 1984.
(19) Liu, Y. S.; Ware, W. R. *J. Phys. Chem.* **1993**, *91*, 5980.
(20) Borsig, E.; Fiedlerová, A.; Hausler, K. G.; Sambatra, R. M.; Michler, G. H. *Polymer* **1993**, *34*, 4787.
(21) Zimerman, O. E.; Weiss, R. G. *J. Phys. Chem. A* **1999**, *103*, 9794.
(22) A photoproduct probably from reaction of traces of molecular oxygen and pyrene in nitrogen-saturated **LDPE**: Brown, G. O.; Zimerman, O. E.; Weiss, R. G. To be published.
(23) Matsui, J.; Mitsuishi, M.; Miyashita, T. *Macromolecules* **1999**, *32*, 386.
(24) The I_1/I_3 ratios from **PY**−**LDPE** (and **PY**−**IPN** derived from **PY**−**LDPE**) cannot be compared rigorously with those from **PYH**−**LDPE** (or **PYH**−**IPN**) due to the presence of an additional, non-pyrenyl lumophore.[22]
(25) Stephen, H.; Stephen, T. *Solubility of Inorganic and Organic Compounds*; Pergamon: New York, 1963; Vol. 1, p 570.
(26) Berlman, I. B. *Handbook of Fluorescence Spectra of Aromatic Compounds*, 2nd ed.; Academic Press: New York, 1971.
(27) Turro, N. J. *Modern Molecular Photochemistry*; University Science Books: Sausalito, CA, 1991, pp 354, 591.
(28) (a) The rate of diffusion in ethanol: Birks, J. B. *Photophysics of Aromatic Molecules*; Wiley: New York, 1970, p 352. (b) The diffusion coefficient in methanol: Castano, F.; Lazaro, A.; Lombrana, S.; Martinez, E. *Spectrochim. Acta* **1983**, *39*, 33.
(29) It is unclear why the decay constant in ethyl acetate is ca. 15% larger than in **PMMA** (or the other media); there may be specific pyrenyl−carboxylate interactions in ethyl acetate that are precluded in the latter by steric factors in **PMMA** and not possible in the other media.
(30) Bloch, D. R.in *Polymer Handbook*, 4th ed.; Brandrup, J., Immergut, E. H., Grulke, E. A., Eds.; Wiley: New York, 1999; VII/497.
(31) Barton, A. F. *Handbook of Polymer Solvent Interaction Parameters*; CRC Press: Boca Raton, FL, 1990, pp 81−88, 161−178, 297−243.
(32) Stannett, V.; Yasuda, H. In *Crystalline Olefin Polymers, Part II*; Raff, R. A. V., Doak, K. W., Eds.; Wiley: New York, 1964; pp 31−184.
(33) Lakowicz, J. R. *Principles of Fluorescence Spectroscopy*; Plenum Press: New York, 1983.
(34) (a) He, Z.; Hammond, G. S.; Weiss, R. G. *Macromolecules* **1992**, *25*, 1568. (b) Jenkins, R. M.; Hammond, G. S.; Weiss, R. G. *J. Phys. Chem.* **1992**, *96*, 496.
(35) Zimerman, O. E.; Cui, C.-X.; Wang, X.; Atvars, T. D. Z.; Weiss, R. G. *Polymer* **1998**, *39*, 1177.
(36) Although the difference between the D_1 and D_2 values for **PYMA**−**IPN** is small, the use of eq 4 seems warranted.

MA0019151